TESTING THE COMPOSITENESS OF QUARKS AND LEPTONS*

M. Abolins
Michigan State University, East Lansing, Michigan 48824

B. Blumenfeld
Johns Hopkins University, Baltimore, Maryland 21218

E. Eichten
Fermi National Accelerator Laboratory, Batavia, Illinois 60510

H. Kagan, K. Lane
Ohio State University, Columbus, Ohio 43210

J. Leveille
University of Michigan, Ann Arbor, Michigan 48109

D. Pellett
University of California, Davis, California 95616

M. Peskin
Stanford Linear Accelerator Center
Stanford University, Stanford, California 94305

J. Wiss
University of Illinois, Urbana, Illinois 61801

One of the major currents of physics in the twentieth century has been the unfolding of structure, the successive analyses of atoms, nuclei, and nucleons into constituent particles with more fundamental equations of motion. It is, then, natural to ask whether quarks and leptons can also be decomposed into simpler constituents. At one time, this idea could be viewed as a casual speculation. But in the past few years, the proliferation of quarks and leptons has become one of the central puzzles of particle physics, and the problem of computing the mass spectrum of quark and leptons has become one of its most difficult challenges. Models in which quarks and leptons are composite have provided a major approach to the resolution of these questions. It is thus important to search for experimental signs of the composite nature of quarks and leptons. In this section, we will compare the abilities of various proposed accelerators to probe for indications of this structure.

We have considered two types of predictions of composite models. The first of these are direct indications of finite radius or internal structure — form factors and other anomalous interactions. The second are new particles suggested by composite models — excited states of quarks and leptons, and fermions of unusual color.

We have based our analysis on the principle of searching for the first signs of compositeness, considering accessible center-of-mass energies to be below the binding energy of quark or lepton constituents. This allows us to approximate the composite quarks and leptons as objects which are almost point-like; the effects of compositeness are summarized as new effective interactions of these point-like objects. It is intuitively clear what some of these interactions must be: One must provide an anomalous magnetic moment, another must add Q^2-dependence to the coupling of the fermion to the photon. We will describe our specific assumptions about these and other interactions in the course of our analysis. But one general remark is appropriate: These new interactions all have their strength characterized by the value of some mass scale. We will consistently use to denote this scale a magnitude Λ which we will refer to as the scale of compositeness. Think of Λ as the energy required to dissociate a composite quark or lepton (in the sense that a proton is dissociated in deep inelastic scattering) or as the reciprocal of the radius of such a composite. It is clear that there is some arbitrariness in the determination of Λ using different effective interactions; this is the same arbitrariness involved in deciding whether f_π or the ρ mass represents the scale of the familiar strong interactions. Our main concern, however, will be to compare the effects of the same interaction term at different accelerators, to determine the values of Λ to which each is sensitive. We will make the assumption that Λ is the same for all quarks and leptons; this is not necessarily true, and the reader should keep that qualification in mind. This method of effective interactions, along with many other aspects of the physics of composite models, has recently been reviewed by Peskin;[1] we will follow the general schema of that paper in formulating our analysis.

Throughout our analysis, we will assume that the standard model is basically correct and that the gauge bosons of the standard model are elementary. There are severe theoretical problems in assuming that the photon or the gluon are composite.[1,2] The $W^\pm$ and Z^0 may be composite. If so, the effects of this will be very striking: The Z^0 will be substantially heavier than in the standard model. A separate "Beyond the Standard Model" report is devoted to the phenomenology of such models.

Direct Probes of Composite Structure

In this section we will concern ourselves with the direct manifestations of the finite size and divisibility of quarks and leptons. We will first examine the effects of quark and lepton form factors. We will then discuss the effects of new contact interactions between quarks and leptons which should appear if these objects have constituents. A striking conclusion of this study is that the search for these contact interactions is actually the most powerful way to test for compositeness; planned e^+e^-, ep, and $p\bar{p}$ facilities are sensitive to values of Λ up to 3 TeV through these effects.

(i) Form Factors

The most stringent bounds on quark and lepton composites which are currently quoted come from bounds on form factors: bounds on electromagnetic form factors from experiments at PETRA, and bounds on the muon and electron (g-2). The PETRA experiments quote[3]

$$\Lambda \geq 100\text{-}200 \text{ GeV} \quad . \qquad (1)$$

(However, as we will explain in section (ii), we believe these experiments place an even tighter bound on Λ.)

*Work supported in part by the Department of Energy, contract number DE-AC03-76SF00515.

The current limits of $\delta a = \frac{1}{2}[(g-2) - (\text{QED value})]$ are:[4]

$$\text{for e:} \quad |\delta a| < 3.2 \times 10^{-10}$$
$$\text{for } \mu\text{:} \quad |\delta a| < 1.5 \quad 10^{-8} \quad . \qquad (2)$$

In composite models, δa is related to the compositeness scale by[5]

$$(\delta a)_\ell = (m_\ell/\Lambda)^2$$

where ℓ is μ or e (this estimate is defended in some detail in Ref. 1), so that the bounds (2) translate into

$$\text{for e:} \quad \Lambda \geq 29 \text{ GeV}$$
$$\text{for } \mu\text{:} \quad \Lambda > 860 \text{ GeV} \quad . \qquad (3)$$

How much can these bounds be improved? Let us discuss first the lepton (g-2) measurements. In both cases an improvement must be made in the accuracy of both theory and experiment. For the electron (g-2) the theory is limited by the accuracy of the numerical evaluation of integrals in the sixth- and eight-order coefficients, and by our knowledge of the value of α. In the past year, a new method for measuring α — the quantized Hall effect[6] — has been discovered, so it is not reasonable to hope for improvement in our knowledge of this quantity. The technique used by the Seattle group[7] to measure the electron (g-2) has not yet reached the limits of its sensitivity. However, it is difficult to imagine improving the current bound of Λ by an order of magnitude. For the muon (g-2), the theoretical uncertainty comes dominantly from diagrams involving the hadronic contributions to light-by-light scattering and vacuum polarization. The accuracy of our knowledge of the former contribution has recently been substantially improved by work of Kinoshita, Nizic, and Okamoto. Improving the accuracy of the latter contribution requires higher-statistics measurements of the e^+e^- annihilation cross section at low energies; these measurements should be done in the next few years using a new high-intensity, low energy e^+ beam available at CERN. These two improvements could decrease the theoretical uncertainty in the muon (g-2) by a factor 10-20.[8] Improvement of the experimental value of the muon (g-2), however, would require building a new facility to replace the CERN muon storage ring. The capabilities and cost of such a new facility have been discussed at this workshop by the Fixed Target group.

To assess the sensitivity of new accelerators to form factor effects, we used the following model for these form factors: Compositeness gives each quark and lepton the same form factor for its coupling to any gauge boson. For $q^2 << \Lambda^2$, one may parameterize this form factor:

$$F_1(q^2) = (1 - q^2/\Lambda^2)^{-1} \approx 1 + q^2/\Lambda^2 \quad . \qquad (4)$$

The same form factor should be used in both the space-like and time-like regions: In hadron physics, the pion form factor extrapolates smoothly from one region to the other if $|q^2| < m_\rho^2$; we expect similar behavior from composite quarks and leptons.

The collaboration proposing an e-p collider for Fermilab has studied the effect on their cross sections of a form factor for the quarks only, at a luminosity of 10^{38}/yr.[9] Their results are presented in Fig. 1. A dedicated e-p collider, at the energy $\sqrt{s} = 2 \times 10^4$ GeV^2 but with a luminosity of 10^{39}/yr., should be able to observe a decrease in the structure functions corresponding to a 10% effect at $Q^2 = (100 \text{ GeV})^2$. Under the assumptions of our model, this would correspond to a bound

$$\Lambda > 600 \text{ GeV} \quad . \qquad (5)$$

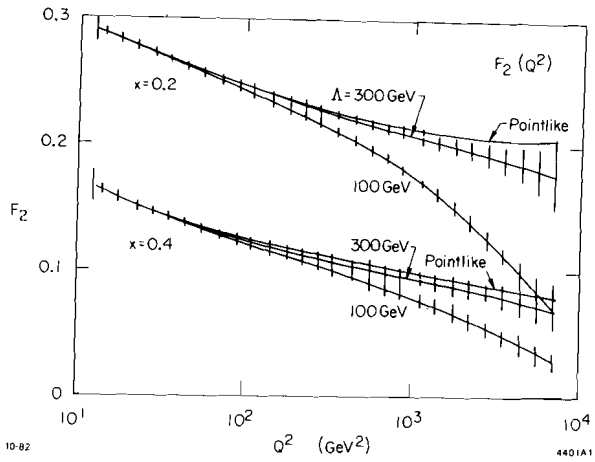

Fig. 1. Effect of a quark form factor on the Q^2 dependence of F_2 on ep scattering, for two values of x. The energies indicated are the values of assumed.

This expectation requires that the high Q^2 structure functions be predicted accurately by QCD evolution of lower Q^2 data. However, this form factor effect is, in principle, distinguishable from QCD scaling violation, since it is independent of x. We should note that we expect this form factor effect, and analogous form factor effects in pp scattering, to be obscured by much larger effects of the contact interactions which we will discuss in section (ii).

One place that the form factor effect should be the dominant one is on the Z^0. Form factors of the form (4) for the coupling of quarks and leptons to the Z^0 will increase the area under the Z^0 peak in any given channel by a factor

$$(1 + 4q^2/\Lambda^2) \quad . \qquad (6)$$

A 10% enhancement in $e^+e^- \to Z^0 \to \mu^+\mu^-$ or in $e^+e^- \to Z^0 \to$ hadrons over the standard model prediction should be striking enough to be credible; this would allow one also to bound

$$\Lambda > 600 \text{ GeV} \quad . \qquad (7)$$

(ii) Contact Interactions

If quarks and leptons are bound states, whatever force binds the constituents will also mediate new interactions between the bound states. One way to visualize these interactions is shown in Fig. 2:

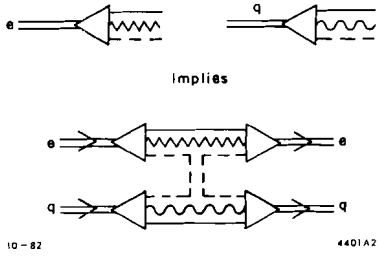

Fig. 2. Origin of an electron-quark contact interaction in a theory of composite quarks and leptons.

Fermion-fermion scattering may be mediated by the exchange of constituents. The diagram shown in Fig. 2 is the precise analogue of a duality diagram representing a scattering process between hadrons. If these constituent-binding interactions are anything like the usual strong interactions, then in fermion-fermion scattering at energies $\sqrt{s} > \Lambda$ one should expect to see

processes characteristic of strong interactions, including multiple production of quarks and leptons and Regge behavior. Cross sections are, of course, scaled down by a geometric factor $(1\ \text{GeV}/\Lambda)^2$; this still gives cross sections of order 1 nb for $s \sim \Lambda \sim 3$ TeV. De Rujula[10] has given a qualitative discussion of quark-quark scattering at energies $s \sim \Lambda$ and has labeled such events "glints."

If $s \ll \Lambda$, however, the effect of these couplings is considerably more subdued. In this regime of energies, the quarks and leptons appear almost point-like and the coupling of Fig. 2 may be approximated, as shown in Fig. 3, by a 4-Fermi interaction:

$$\delta\mathscr{L} = C\,(\bar{e}e)(\bar{q}q) \quad . \tag{8}$$

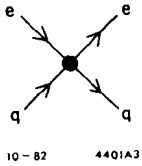

Fig. 3. Phenomenological description of the contact interaction valid for $s < \Lambda^2$.

A first question is the magnitude of the coefficient C giving the strength of this interaction. This coefficient has the dimensions of $(\text{mass})^2$. If Fig. 2 showed a process in hadron physics, mediated by meson exchanges, the appropriate value of C would be (g_ρ^2/m_ρ^2), where $(g_\rho^2/4\pi) = 2.1$. We will thus estimate C by:

$$C = \pm g^2/\Lambda^2 \quad , \quad g^2/4\pi = 1 \quad . \tag{9}$$

A more difficult question is that of the space-time structure of this 4-Fermi interaction. Assuming that this coupling is a correction to the standard model, the structure of this interaction should respect $SU(3) \times SU(2) \times U(1)$. (Since Λ is well above the scale of weak interaction symmetry breaking, $SU(3) \times SU(2) \times U(1)$ should be a manifest symmetry.) If Λ is taken smaller than 10 TeV, this coupling must also conserve quark and lepton flavors; otherwise it will lead to unacceptably large rates for processes such as $\mu \to e\gamma$ and $K^0 \to \mu e$.[1,5] However, these two constraints are not very restrictive. The complete set of 4-Fermi interactions (for lepton-lepton processes only) satisfying these restrictions is presented in Appendix A. One should note two features of this collection of interactions: First, these interactions generally violate parity. There is no reason why they should not; the left- and right-handed electron are completely different species above the scale of $SU(2) \times U(1)$ breaking. Secondly, the list of possible interactions contains terms usually thought of as scalar, pseudoscalar, and tensor weak exchanges.

Since the list in Appendix A is so long and since all of the coefficients appearing there are unknown, we felt that the most general interaction is too unwieldly for consideration in a summer study. We have, therefore, restricted our attention to consideration of a single term in the effective interaction; we believe that the physics of this term is sufficiently rich to display the basic consequences of the full effective interaction. Our model is to take as the contact interaction a flavor-diagonal left-handed current:

$$\begin{aligned}\delta\mathscr{L} = A\frac{g^2}{\Lambda^2}\Big\{&\frac{1}{2}(\bar{e}_L\gamma^\mu e_L)(\bar{e}_L\gamma_\mu e_L) \\ &+ (\bar{e}_L\gamma^\mu e_L)(\bar{\mu}_L\gamma_\mu \mu_L) + (\bar{e}_L\gamma^\mu e_L)(\bar{q}_L\gamma_\mu q_L) \\ &+ \frac{1}{2}(\bar{q}_L\gamma^\mu q_L)(\bar{q}_L\gamma_\mu q_L) + \ldots\Big\}\end{aligned} \tag{10}$$

where A may be ± 1. One should note that this interaction embodies the assumption that all quarks and leptons contain common constituents. If two species of fermion (e.g., e and t) have no common constituents, their contact interactions will be suppressed. (This suppression would be analogous to the Zweig's rule suppression of processes in the familiar strong interactions.) We can be assured, however, that as long as electrons and quarks are composite, the contact interaction will operate with full strength in Bhabha scattering and in quark-quark hard scattering, processes in which the four fermions involved are identical.[11]

These new contact interactions turn out to be very sensitive probes of composite structure. The reason for this is apparent from Fig. 4, which shows the contributions to $e^+e^- \to \bar{q}q$, including standard model effects and the contact interactions. Since the contact

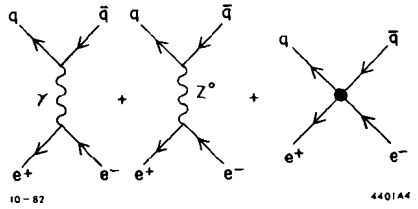

Fig. 4. Contributions to $e^+e^- \to \bar{q}q$ in composite models.

interaction is a strong interaction competing with interactions of electromagnetic strength the relative size of the deviation from standard model is

$$\left(\frac{g^2}{\alpha\Lambda^2}\right) \quad . \tag{11}$$

The effect of the contact interaction is thus larger by a factor of α than the form factor effect; recognition of the effects of the contact interaction increases the value of Λ to which a given experiment is sensitive by a factor of $\sqrt{\alpha} \approx 10$![11]

This line of reasoning leads us to reinterpret the PETRA bound on the electron form factor quoted in (1) as a bound

$$\Lambda > .75\ \text{TeV} \quad . \tag{12}$$

We will defend this estimate in detail in a moment. In neutrino scattering an (admittedly, more model-dependent) estimate from the existing data gives a stronger bound: If one grants that anomalous currents make up less than 10% of the ν-hadron neutral current total cross section (otherwise, one is hard-pressed to explain the small derivation of the ρ parameter from 1), one finds a bound

$$\left(\frac{4m_Z^2}{\alpha\Lambda^2}\right) < .1 \tag{13}$$

that is

$$\alpha\Lambda^2 > (200\ \text{GeV})^2 \quad \text{or} \quad \Lambda > 2.5\ \text{TeV} \quad . \tag{14}$$

An additional moral to be drawn from this estimate is that, in composite models, unusual currents of the types presented in Appendix A could easily appear in low-energy weak interaction processes at the 10% level.

Before we apply the contact interaction (10) to processes at proposed accelerators, we should say a few words about the multiple production of quarks and leptons, the process shown in Fig. 5a. If the constituent-binding interactions are similar to the familiar strong interactions, this process will be a major contribution to the total cross section if $s > \Lambda$. However, we have just seen that Λ is a very large scale; hence, we should concentrate on the case $s < \Lambda$. In this case, the multiple production process should be represented by the local interaction shown in Fig. 5b. This is a 6-fermion coupling. If one imposes the constraint that this coupling conserve helicity (an assumption required in composite models to allow quark

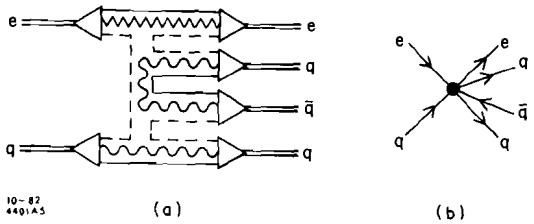

Fig. 5. Multiple production of quarks and leptons.

and lepton masses to be much smaller than Λ),[1] the simplest such couplings correspond to local operators with dimensions $(\text{mass})^{10}$, requiring a coefficient with dimensions $(\text{mass})^{-6}$. A typical effective interaction of this type is:

$$\frac{1}{\Lambda^6}\left[\partial^\mu(\bar{e}_L e_R)\right]\ (\bar{q}_R q_L)\ (\bar{q}_L \gamma_\mu q_L) \quad . \tag{15}$$

Such an interaction leads to a cross section

$$\sigma(eq \to eq\bar{q}q) \sim \frac{1}{\Lambda^2}\left(\frac{s}{\Lambda^2}\right)^5 \quad , \tag{16}$$

so the multiple-production cross section turns on extraordinarily slowly with energy. We should note that De Rujula's estimates of multiple production[10] assumed a considerably more mild s-dependence.

Let us now investigate the consequences of the interaction (10) at various planned accelerators. A compilation of the specific cross sections we have used is given in Appendix B. The effect is most straightforward to discuss at ep machines, where an electron-quark coupling causes in a straightforward way an apparent change in the value of the structure functions at large Q^2. In our discussion of form factors we claimed that a 10 × 1000 GeV ep collider with a luminosity of 10^{39}/yr., could detect a 10% deviation of the structure functions from QCD predictions at $Q^2 = (100\ \text{GeV})^2$. The contact interaction (10) makes an effect smaller than this only if

$$(\alpha\Lambda^2) > (350\ \text{GeV})^2 \quad \text{or} \quad \Lambda > 4\ \text{TeV} \quad . \tag{17}$$

In e^+e^- annihilation, one can observe the effects of the contact interaction by searching for a deviation from electroweak predictions in wide-angle Bhabha scattering. We might first discuss the sensitivity of current experiments. Figure 6 shows the effect of the interaction (10), and contact interactions with other space-time structures, on the angular distribution of Bhabha scattering at $\sqrt{s}$ = 35 GeV. The Mark J experiment[12] has measured the Bhabha scattering cross section at this energy with an accuracy of ±5% (including an estimate of 3% systematic uncertainty) and found agreement with the predictions of the standard model; this measurement already excludes values of Λ up to .75 TeV. (This justifies our Eq. (12).) We should emphasize that this experiment does not require an absolute measurement of the value of the cross section: Since the contact interaction makes a negligible effect at small angles, one can normalize to the QED prediction there.

This result is easy to extrapolate to higher-energy e^+e^- machines. Just on the Z^0 peak, the contact interactions is obscurred by the overwhelming effect of the resonance. One does not have to go far on either side of the peak, however, to find a significant effect. Figure 7 shows the Bhabha scattering cross section at $\sqrt{s}$ = 100 GeV. The cross section at large angles is only one-fifth as large at this energy as at PETRA energies, but still a 5% determination of the cross section at 90° should be possible. This measurement would be sensitive to Λ unless

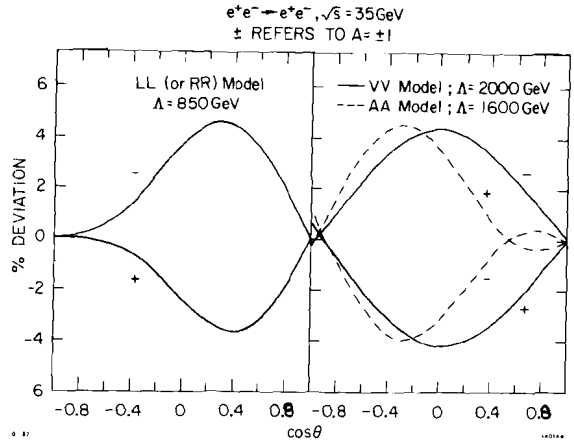

Fig. 6. Deviation of the cross section for $e^+e^- \to e^+e^-$ from that of the standard electroweak theory, due to compositeness of the electron, computed for $\sqrt{s}$ = 100 GeV. The LL model is that of Eq. (10). The RR, VV, and AA models are obtained by replacing the left-handed currents in Eq. (10) by right-handed, vector, and axial-vector currents, respectively. (From Ref. 11)

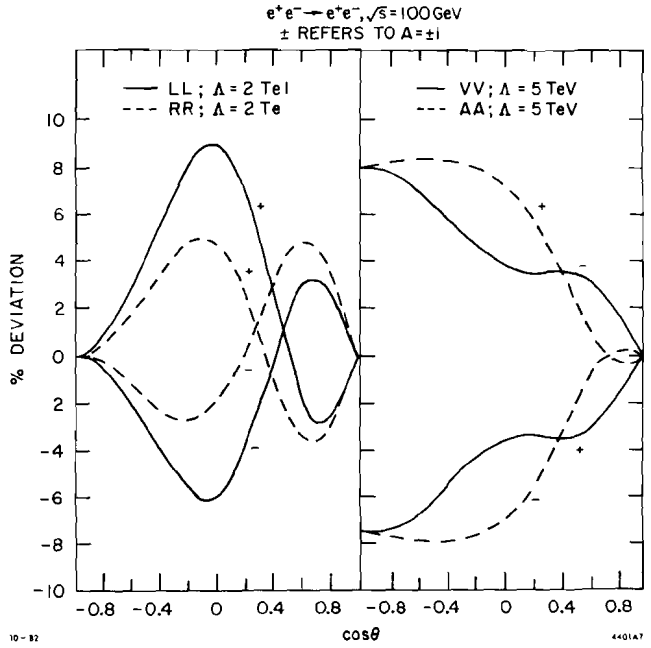

Fig. 7. Deviation for the cross section of $e^+e^- \to e^+e^-$ from that of the standard electroweak theory, computed for $\sqrt{s}$ = 100 GeV. The notation is as in Fig. 6. We have set m_Z = 93.0 GeV, Γ_Z = 2.9 GeV. (From Ref. 11)

$$\Lambda > 2\ \text{TeV} \quad . \tag{18}$$

If electrons and muons can exchange constituents, one should also see a deviation from the standard model prediction for $\sigma(e^+e^- \to \mu^+\mu^-)$. The magnitude of this effect, computed for Λ = 3 TeV, is shown in Fig. 8. The effect is a 10% correction to the standard model result at $\sqrt{s}$ = 110 GeV, but it gives only a very small correction below the resonance.

One can test quark compositeness in hadron colliders by searching for the effects of (10) on the production of light quark jets with large transverse momentum (p_T). At sufficiently high p_T the dominant QCD process for jet production should be hard scattering of quarks by the exchange of a single gluon. In high p_T $p\bar{p}$ collisions, this process involves mainly the

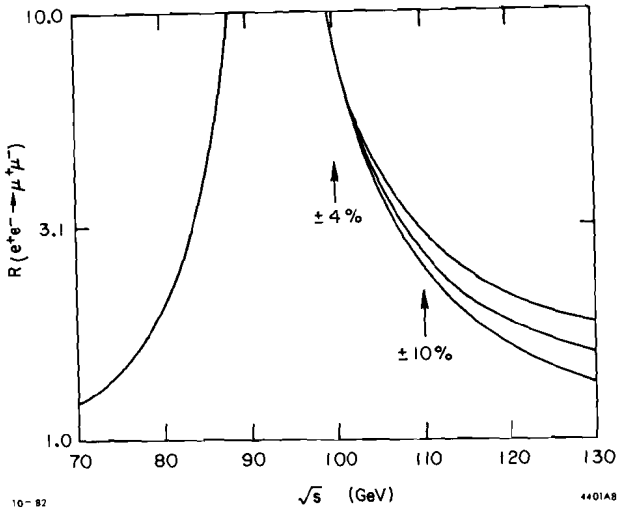

Fig. 8. Deviation of the cross section for $e^+e^- \to \mu^+\mu^-$ from that of the standard electroweak theory, due to the compositeness of leptons, computed for $\Lambda = 3$ TeV and $A = \pm 1$.

valence quarks and is the analogy of Bhabha scattering in the e^+e^- case. The diagrams for $q\bar{q} \to q\bar{q}$ scattering including a contact term are shown in Fig. 9.

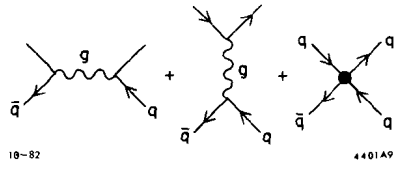

Fig. 9. Diagrams for $q\bar{q} \to q\bar{q}$ scattering in composite models.

For pp colliders, the dominant process in high p_T $q_iq_j \to q_iq_j$ scattering, including a contact term, is shown in Fig. 10. Of course, at experimentally accessible p_T's, all the processes $q_i\bar{q}_j \to q_i\bar{q}_j$, $q_i\bar{q}_i \to q_j\bar{q}_j$, $\bar{q}_i\bar{q}_j \to \bar{q}_i\bar{q}_j$, $\bar{q}_ig \to q_ig$, $q_ig \to q_ig$, and $gg \to q_i\bar{q}_i$ (for $q_1 = u$, $q_2 = d$) contribute to the jet production cross section background. All these cross sections, including the effects of a composite contact term of the form

$$4\pi A/2\Lambda^2 \; (\bar{u}_L\gamma^\mu u_L + \bar{d}_L\gamma^\mu d_L)\; (\bar{u}_L\gamma^\mu u_L + \bar{d}_L\gamma^\mu d_L) \quad ,$$

are tabulated in Appendix B (Eq. (B.8)). (We ignore the effect of a form factor at the quark-quark-gluon vertex; this is smaller than the effect of the contact interaction by a power of α_s.) The associated jet production cross section is given by:

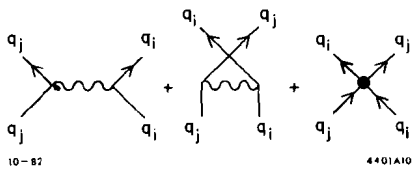

Fig. 10. Diagrams for $qq \to qq$ scattering in composite models.

$$\frac{d\sigma}{d\,p_T\,dy} = \sum_{\substack{ij=\\1,5}} \int_{\frac{4p_\perp^2}{s}}^{1} d\tau \; \frac{2p_T}{|\cos\theta_{CM}|} \int_\tau^1 dx \qquad (19)$$

$$\left[\frac{f_i(x,p^2)\; f_j(\tau/x,p_T^2) + f_j(s,p_T^2)\; f_i(\tau/x,p_T^2)}{(1+\delta_{ij})}\right]$$

$$\frac{\pi}{\tau^2 s^2}\left\{\frac{d\hat{\sigma}^{ij}}{d\hat{t}}\Big|_{\hat{t}_+}\delta(x-x_+) + \frac{d\hat{\sigma}^{ij}}{d\hat{t}}\Big|_{\hat{t}_-}\delta(x-x_-)\right\}$$

where

$$\sin\theta_{CM} = \frac{2p_T}{\sqrt{\tau s}} \quad ;$$

$$x_\pm = \tau^{1/2}\left\{\frac{\sqrt{s}}{2p_T} \pm \left(\frac{s}{4p_T^2} - \frac{1}{\tau}\right)^{1/2}\right\} \quad ;$$

$$\hat{t}_\pm = -\frac{\tau s}{2}\left(1 \mp \left(1 - \frac{4p_T^2}{\tau s}\right)^{1/2}\right) \quad ;$$

and $d\hat{\sigma}_{ij}/d\hat{t}$ is the differential cross section for the subprocess. $f_1 = u$, $f_2 = d$, $f_3 = \bar{u}$, $f_4 = \bar{d}$, $f_5 = g$ are various parton distribution functions; y is the rapidity of the jet and p_T is its transverse momentum. The distribution functions include scale violating effects associated with the scale p_T.

The effect of the contact term for various values of Λ and $A = \pm 1$ is shown in Fig. 11a for a $p\bar{p}$ collider at $\sqrt{s} = 2$ TeV and in Fig. 11b for a pp collider at the same $\sqrt{s}$. Under the assumption that detection of a variation from QCD expectations would be possible if the variation is: 1) at least a factor of two, 2) gives at least a 100 events/yr variation from expectation, and 3) gives a detectable non-scaling energy behavior; it should be possible to observe a contact term in pp colliders with $\sqrt{s} = 2$ TeV up to a $\Lambda \sim 1.5$ TeV and in a pp collider at the same energy a somewhat higher scale may be probed $\Lambda \gtrsim 2.0$ TeV. The better limit for a pp machine is due to the large luminosity possible there (assumed to be a factor of 1000 better than $p\bar{p}$). In both the pp and $p\bar{p}$ cases a

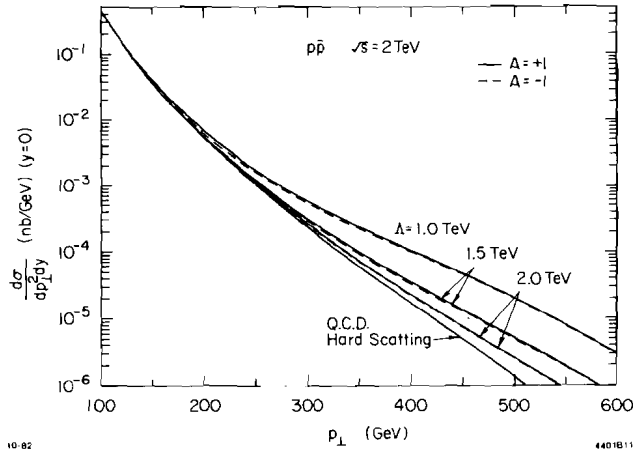

Fig. 11a. Jet production cross section in a theory with composite left-handed quarks in $p\bar{p}$ scattering, $\sqrt{s} = 2$ TeV. (From Ref. 11)

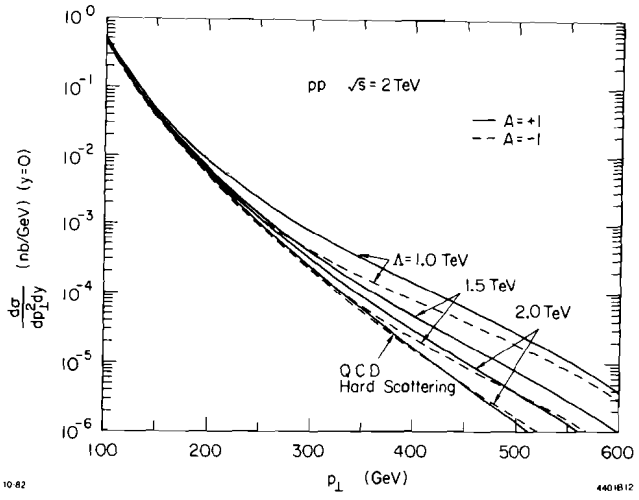

Fig. 11b. Jet production cross section in a theory with composite left-handed quarks in pp scattering, $\sqrt{s}$ = 2 TeV. (From Ref. 11)

more detailed study needs to be done of what constitutes an experimentally identifiable deviation from ordinary hadronic behavior.

Finally, if both light quarks and muons are composite then the effects of the associated contact term (10) will modify the usual Drell-Yan cross section. The resulting differential cross section for muon pairs of mass squared $\hat{s} \equiv \tau s$ and Feynman $x_F = 0$ is:

$$\left.\frac{d\sigma}{dx_F\, d\sqrt{\tau}}\right|_{x_F=0} = u(\sqrt{\tau};\tau s)\ \bar{u}(\sqrt{\tau},\tau s)\ \hat{\sigma}(u\bar{u} \to \mu^+\mu^-) + d(\sqrt{\tau};\tau s)\ \bar{d}(\sqrt{\tau},\tau s)\ \hat{\sigma}(d\bar{d} \to \mu^+\mu^-) \quad . \tag{20}$$

The cross section for the subprocess $\hat{\sigma}$ is given in Appendix B (Eq. (B.6)). The results for various Λ and $A = \pm 1$ are presented in Fig. 12. Again assuming the conditions necessary for observing the effects of the contact term are: 1) A factor of two deviation from the expected Drell-Yan cross section, 2) at least 100 $\mu^+\mu^-$ events/yr effect and 3) observable non-scaling energy behavior of the events; the limit set on Λ by a $p\bar{p}$ collider at $\sqrt{s}$ = 2 TeV should be at least 4 TeV.

It is amusing to consider the effects of (10) at still higher energies. An e^+e^- collider which can reach $\sqrt{s}$ = 1 TeV may be seen to be sensitive to

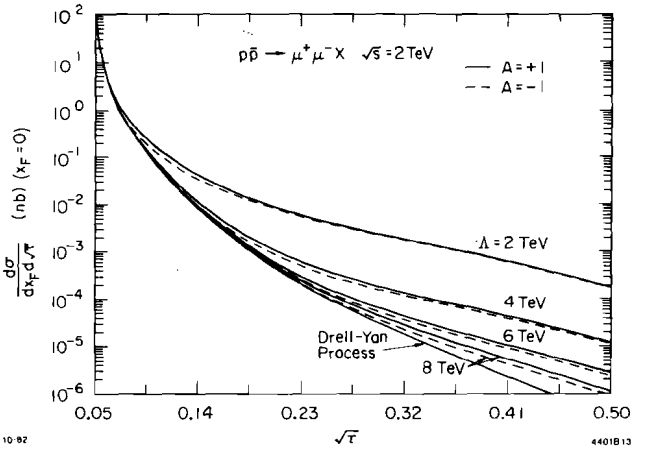

Fig. 12. μ pair production cross section in a theory with composite left-handed quarks, computed for $p\bar{p}$ scattering $\sqrt{s}$ = 2 TeV. (From Ref. 11)

$\Lambda \sim 30$ TeV (Fig. 13). But it is much more instructive to consider the cross sections which would be observed at such a machine if, as is certainly possible, Λ is in the range of a few TeV. Figure 14 shows the cross section for $e^+e^- \to \mu^+\mu^-$, in units of R over the range of such a machine, for Λ = 3 TeV and Λ = 6 TeV. Figure 15 displays this cross section over a larger range for the case Λ = 3 TeV. Here the μ pair cross section displays real strong interaction physics. The rate is 10^3 times the standard model prediction.

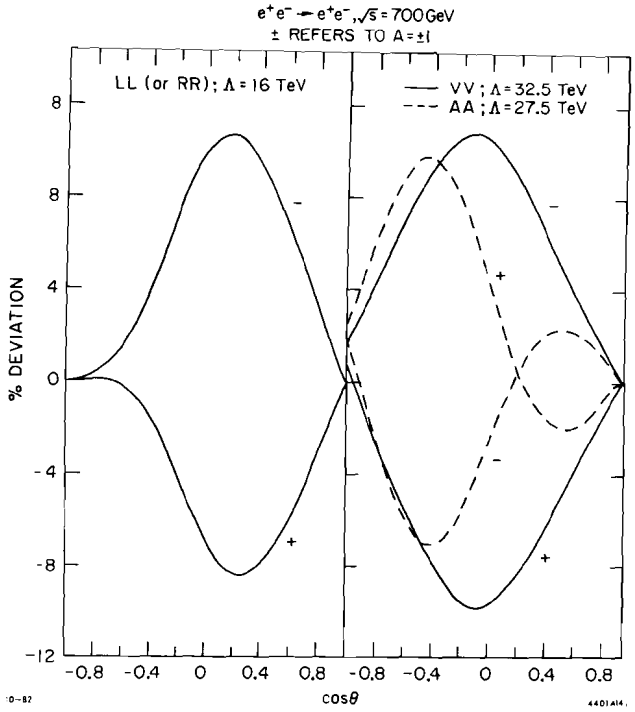

Fig. 13. Deviation of the cross section for $e^+e^- \to e^+e^-$ from that of the standard electroweak theory, due to compositeness of the electron, for $\sqrt{s}$ = 700 GeV. The notation is as in Fig. 6. (From Ref. 11)

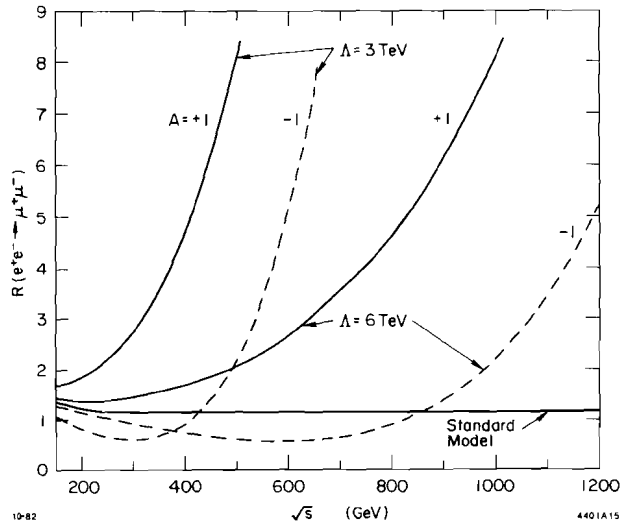

Fig. 14. $R(e^+e^- \to \mu^+\mu^-)$ in a theory with a composite left-handed electron.

Let us, however, return to more readily accessible energies, to tabulate the sensitivity to Λ which can be obtained by various techniques before 1992.

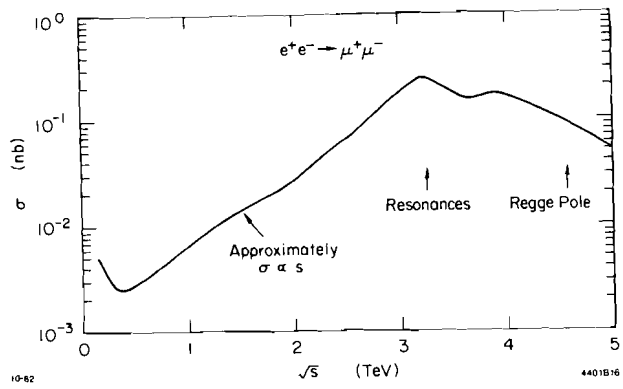

Fig. 15. Sketch of $\sigma(e^+e^- \to \mu^+\mu^-)$ in very high energy e^+e^- collisions, for $\Lambda \sim 3$ TeV.

This compilation, the conclusions of our study, is given in Table I. If quarks and leptons are indeed composites of particles bound with energies of a few TeV, that fact will become clear in many ways within the next ten years.

Table I. Conclusions: Compositeness Limits* by 1992

Process	$\Lambda \geq$	Subprocess Tested
Muon (g-2)	3 TeV	
ep, 10 × 1000, 10^{39}/yr	4 TeV	eq → eq
e^+e^-, $\sqrt{s} \leq 100$ GeV, 10^{38}/yr	2 TeV	$e^+e^- \to e^+e^-$
e^+e^-, $\sqrt{s} \geq 200$ GeV, 10^{38}/yr	3 TeV	$e^+e^- \to e^+e^-$
pp, $\sqrt{s}$ = 2 TeV, 10^{40}/yr	2 TeV	qq → qq
$p\bar{p}$, $\sqrt{s}$ = 2 TeV, 10^{37}/yr	1.5 TeV	qq → qq
$p\bar{p}$, $\sqrt{s}$ = 2 TeV, 10^{37}/yr	4 TeV	$\bar{q}q \to \mu^+\mu^-$

Note: These estimates assume the possibility of constituent exchange in the indicated subprocesses. Such exchanges might be suppressed in processes involving non-identical flavors.

*Or compositeness discovery.

New Particles Predicted by Composite Models

In this section we will discuss the production of a variety of particles predicted by composite models. If quarks and leptons are composite, there should be excited states of these particles which decay back to the ground state by emitting a photon or a gluon. If the constituents are colored (so that a lepton corresponds to a color-singlet bound state of colored objects) one can also imagine forming excited states by rearranging the relative color orientation of the constituents. Thus, one should expect some excited states of quarks and leptons to belong to higher representations of color.

Any of these excited states may be pair-produced in Z^0 decay or e^+e^- annihilation. Any of these objects which are colored may be pair produced in gluon-gluon or photon-gluon fusion. The rates for such pair-production processes are the same as for any elementary fermion with the same mass and quantum numbers.

In addition, those excited states which can decay by emission of a photon or a gluon can also be created by the inverse process. Such states may thus be singly produced in quark-gluon collisions or produced in association with a light quark or lepton in e^+e^- annihilation or Z^0 decay. However, both the production and decay processes involve couplings of the magnetic moment type; the rates are thus extremely sensitive to Λ, being proportional to Λ^{-4}.

We should, then, discuss the production of these excited states under two different hypotheses for Λ: (The reader should recall that the value of Λ parameterizing a magnetic moment coupling may differ by factors of two from the value which parameterizes the processes discussed in section (i).)

(1) Λ is relatively small. In this case the magnetic moment couplings are important effects, and excited quarks and leptons decay relatively rapidly by photon or gluon emission. In our rate computation, for all machines, we have used the lowest imaginable value, Λ = 300 GeV. The production rates may be scaled to any other value of Λ by multiplying by $(300 \text{ GeV}/\Lambda)^4$.

(2) Λ is very large. In this case, the magnetic moment couplings yield negligible production rates; only the pair production of excited states is relevant. The decay rates of these excited states also decrease as Λ^{-4}, whether the dominant decays proceed by magnetic moment effects or by 4-fermion contact interactions. If $\Lambda \sim 100$ TeV (this is the lowest value of Λ allowed if $\mu \to e\gamma$ can proceed by rearrangement of lepton constituents), these excited states have lifetimes $c\tau \sim 1$ cm. One could thus tolerate very low rates for the pair production process, because the signature of a stable heavy particle would be so dramatic.

We will therefore divide this section into three main parts. In the first two we examine the cross sections for the production of excited states of quarks and leptons in various reactions, for cases (1) and (2) respectively. In the last subsection we will discuss the signatures and decay characteristics of these new states.

(i) The Case of Small Λ:

If Λ is small, the single production of excited objects will dominate over the pair production. The vertices necessary for the computations of the single-production cross sections are shown in Fig. 16. They are all of the magnetic type, as required by gauge invariance. We will present the cross sections for a variety of single-production processes.

Let us first consider the production of excited leptons in e^+e^- annihilation. For simplicity we do not consider the production of an excited electron, but rather an excited μ or τ. The relevant diagrams for these latter processes are shown in Fig. 17; only diagrams with a photon in the s-channel contribute. Assuming $\sin^2\theta_W = .25$ for simplicity we easily find the production rate

$$\sigma = \frac{2\pi\alpha^2}{3}\frac{m_*^2}{4}\frac{(s-m_*^2)^2(s+2m_*^2)}{s^3} \cdot \left\{1 + \frac{16}{9}\frac{s^2}{(s-m_Z^2)^2 + m_Z^2\Gamma_Z^2}\right\} \quad (21)$$

where m_* is the excited lepton mass, and all other lepton masses have been set to zero. The cross section is relatively flat as a function of m^* for fixed s; for s = 200 GeV, Λ = 300 GeV $\sigma(e^+e^- \to ff^*) \sim$ (.1 - .2 pb). Excited quarks are singly produced at roughly the same level.

Excited lepton production

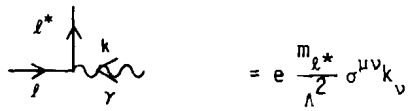

$$= e \frac{m_{\ell^*}}{\Lambda^2} \sigma^{\mu\nu} k_\nu$$

Excited quark production

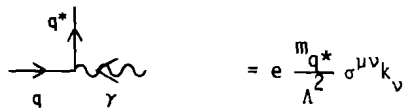

$$= e \frac{m_{q^*}}{\Lambda^2} \sigma^{\mu\nu} k_\nu$$

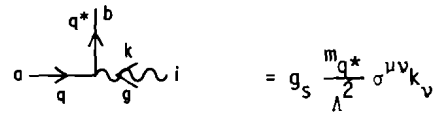

$$= g_s \frac{m_{q^*}}{\Lambda^2} \sigma^{\mu\nu} k_\nu \, (\tau^i)_{ab}$$

Color sextet production

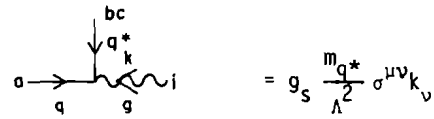

$$= g_s \frac{m_{q^*}}{\Lambda^2} \sigma^{\mu\nu} k_\nu \, \frac{1}{2} (\tau^i)_{ad} \, \epsilon^{dbc}$$

Color octet production

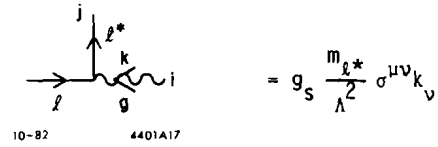

$$= g_s \frac{m_{\ell^*}}{\Lambda^2} \sigma^{\mu\nu} k_\nu \, \delta^{ij}$$

Fig. 16. Vertices for excited fermion productions.

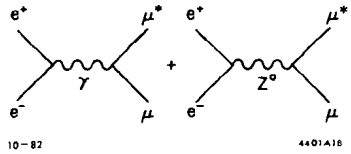

Fig. 17. Diagrams for $e^+e^- \to \mu^+\mu^{*-}$.

Any excited fermion which is sufficiently light may also be produced in Z^0 decays. The branching ratio for production of an excited fermion f*, together with an $\bar{f}$, is most conveniently expressed by comparing it to the branching ratio to $f\bar{f}$. For any fermion f (assuming the simple couplings of Fig. 15):

$$\frac{BR(Z^0 \to f^*\bar{f})}{BR(Z^0 \to f\bar{f})} = \frac{1}{2} \frac{m_*^2 m_Z^2}{\Lambda^4} \left(1 - \frac{m_*^2}{m_Z^2}\right)^2 \left(1 + \frac{2m_*^2}{m_Z^2}\right) . \tag{22}$$

This ratio is plotted in Fig. 18 for m_Z = 93 GeV; it is substantial almost to the edge of the kinematically allowed region.

Let us now turn to the hadronic production of a single excited quark, q*. In principle, one can produce both color triplet and color sextet objects; the difference in the cross sections is only a color factor. So we consider the production of a color triplet q* by the process gluon + q → q* as illustrated in Fig. 19. To find the cross sections for color sextets, multiply the following results by 2.5.

Neglecting the width of the q*, we easily find

$$\sigma = \frac{2\pi^2}{3} \frac{m_*^4}{\Lambda^4} \frac{1}{s} \int_{\ell n \sqrt{\tau}}^{\ell n \, 1/\sqrt{\tau}} dy \tag{23}$$

$$\alpha_s \left[G\left(x_1, m_*^2\right) Q\left(x_2, m_*^2\right) + (x_1 \leftrightarrow x_2) \right]$$

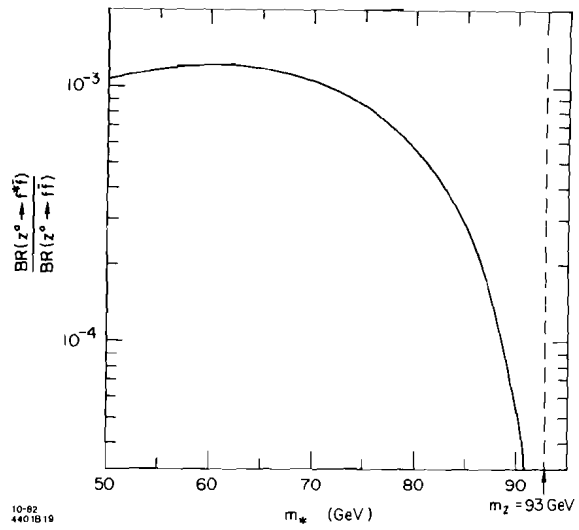

Fig. 18. The ratio of branching ratios $BR(Z^0 \to f^*\bar{f})/BR(Z^0 \to f\bar{f})$, as a function of the mass of the f*, using Λ = 300 GeV.

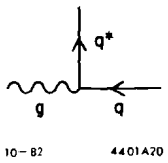

Fig. 19. Mechanism for single excited quark production in hadron-hadron collisions.

where $\tau \equiv m_*^2/s$, G is the gluon distribution function, and Q is the quark distribution function. We have plotted the production cross sections for various energies in pp and $p\bar{p}$ collisions in Fig. 20 for the case Λ = 300 GeV. Note that these cross sections are very flat with increasing mass. It is difficult to give reliable rates for higher energies since the gluon and valence or quark distributions are being probed at

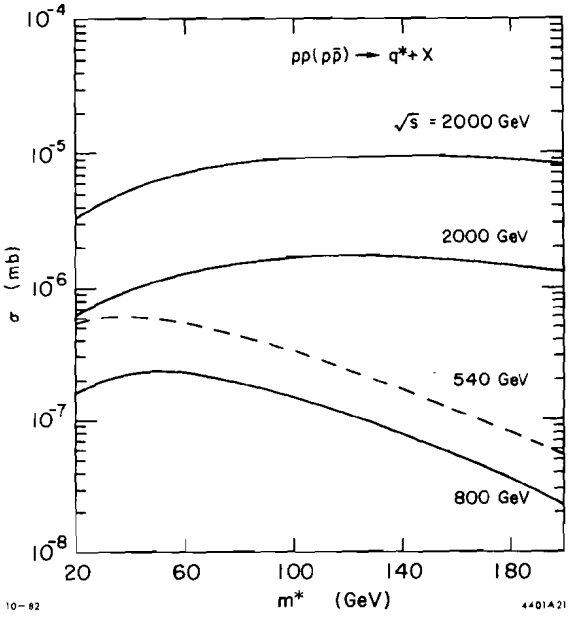

Fig. 20. Cross sections for production of a single excited quark of mass m* in pp (solid lines) and $p\bar{p}$ (dashed lines) collisions. We have taken Λ = 300 GeV.

$\sqrt{\tau} \approx \sqrt{\mu^2}/s \sim 10^{-2} - 10^{-1}$ for already $\sqrt{s} = 2000$ GeV, and the sharp rise due to scaling violations leads to significant uncertainty for very small x. We shall return later to the expected signatures for detection of these objects. Note, however, that with an integrated luminosity of $10^{40}/cm^2$ and $m_* = 200$ GeV, one expects 10^5 events/yr at $\sqrt{s} = 800$ GeV in a proton machine.

Finally, we turn to the example of a single produced lepton in the octet representation of color. This amusing object could be produced in lepton-proton collisions by the process shown in Fig. 21. The cross section is easily calculated to be:

$$\sigma = \frac{4\pi^2}{s}\frac{m^{*4}}{\Lambda^4}\alpha_s(m^{*2})\, G\left(\frac{m^{*2}}{s}, m^2\right) \quad . \qquad (24)$$

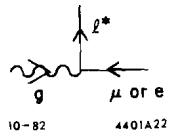

Fig. 21. Mechanism for the production of a color-octet excited lepton.

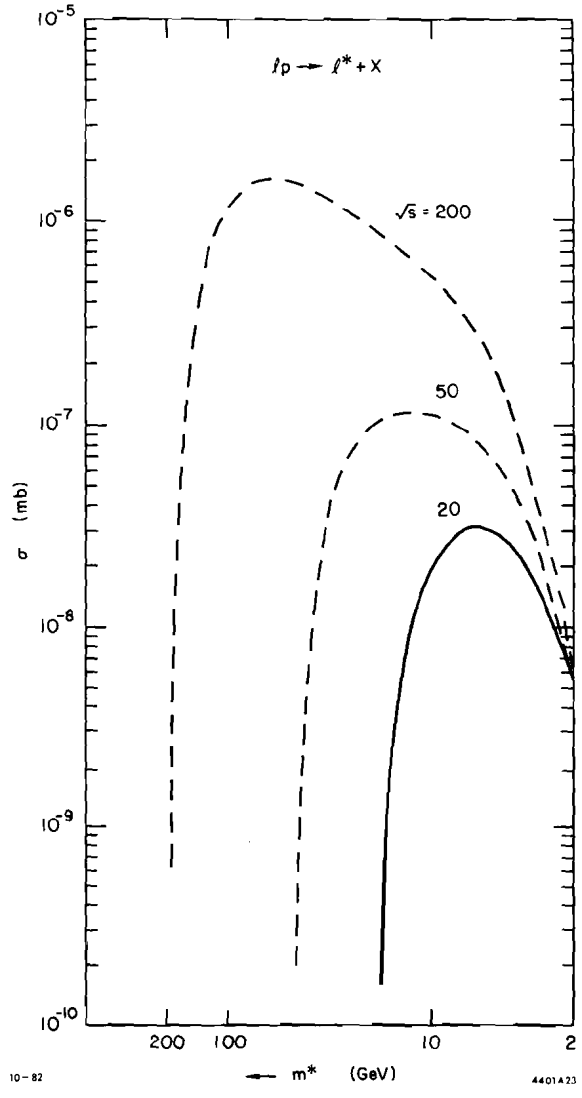

Fig. 22. Cross sections for production of a color-octet excited lepton in lepton-proton collisions, for various values of $\sqrt{s}$ and Λ = 300 GeV.

Since muon beams presently exist with $E_\mu \approx 200$ GeV, and beams with $E_\mu \sim 1000$ GeV might be available soon we plot this cross section in Fig. 22 for $\Lambda = 300$ GeV and $\sqrt{s} =$ 20, 50 GeV. The cross section for an ep machine (10 GeV electrons colliding with 1 TeV proton leading to a $\sqrt{s} = 200$ GeV) are also plotted in Fig. 22.

In the curves of Fig. 22, the sharp rise and fall mirror the rise and fall of the gluon distribution at small and large x, with scaling violations. Due to the large uncertainty in this distribution there may be large errors in these cross sections; let the reader beware!

(ii) The Case of Large Λ

Although the rates for single production of excited fermions displayed in section (i) were quite large, one must remember that these rates decrease rapidity, proportional to Λ^{-4}, as Λ increases. If Λ is of order 10 TeV, rather than 300 GeV, the processes discussed in section (i) would be invisible. However, the rates for pair-production of excited states are independent of Λ and limited only by phase space. These become the dominant production processes when Λ is large.

If $\Lambda >> s$, the cross sections for pair production of excited fermions is the same as for pair production of elementary fermions with the same electromagnetic, weak, and color quantum numbers. Fermions of electric charge Q contribute Q^2 units of R to the e^+e^- annihilation cross section for $s > 4m^{*2}$. If $2m^* < m_Z$, the branching ratio of the Z^0 into such fermion pairs is several percent; the precise formula (omitting the standard phase space factor) is:

$$\Gamma(Z \to f\bar{f}) = (90 \text{ MeV}) \cdot 8 \cdot [I_3 - Q \sin^2\theta_W]^2 \quad (26)$$

for each color and handedness (R or L), where I_3 is the weak isospin and Q is the electric charge. Thus, if excited fermions have modest masses, they will be produced copiously at an e^+e^- collider.

Excited fermions which are colored may also be produced in hadronic collisions; here they represent a smaller fraction of the total cross section, but higher mass states are accessible. The rates may be estimated using the standard lore of perturbative QCD. The diagrams which lead to the production of a pair of colored fermions are shown in Fig. 23. The relevant formulae for the cross sections are lengthy and will not be reproduced here. They may be found in Ref. 13.

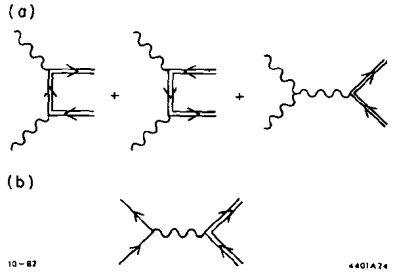

Fig. 23. The perturbative diagrams for the pair production of excited colored objects.

The production cross sections for excited fermions are plotted in Fig. 24 (a-d) for proton-proton collisions at $\sqrt{s} = .8$, 2, 10, 40 TeV. Because the gluon fusion diagrams dominate over the kinematic range considered, these results also apply to $p\bar{p}$ collisions. Again, one must be careful in using these curves. Charm production is not very well described by perturbative calculation of the type described above. However, in all cases known, perturbative calculations underestimate the actual rates. Greater caution must

be exercised, however, when $x \equiv m^2/s$ is either very small $x \lesssim .05$ or very large $x \gtrsim .5$. In these latter cases, errors of an order of magnitude could result from the parameterization of the gluon distribution. Our knowledge of perturbative QCD is not advanced enough to permit a better evolution of these cross sections and the reader should consider them only as a guide. With all the caveats, however, it does seem that the rates are extremely large (due to large color factors) especially for color sextet and decouplet quarks. The signatures of these objects will make them rather easy to detect as we shall see in the next section.

As a quick guide, we can also give a rule of thumb to predict the production rate of one color object when given that of another. Indeed in the kinematic region we are exploring, the gluon fusion diagrams dominate, as we have already emphasized. In the integration of these diagrams, a term of the form $c_1 \cdot \ln(s/m^2)$ arises from the propagator, where c_1 is a color factor. This logarithmic term dominates the cross section. Consequently the cross sections are in the ratios of c_1 for the various color representations:

color =	3	;	6	;	8	;	10
c_1 =	16/3	;	200/3	;	72	;	360 .

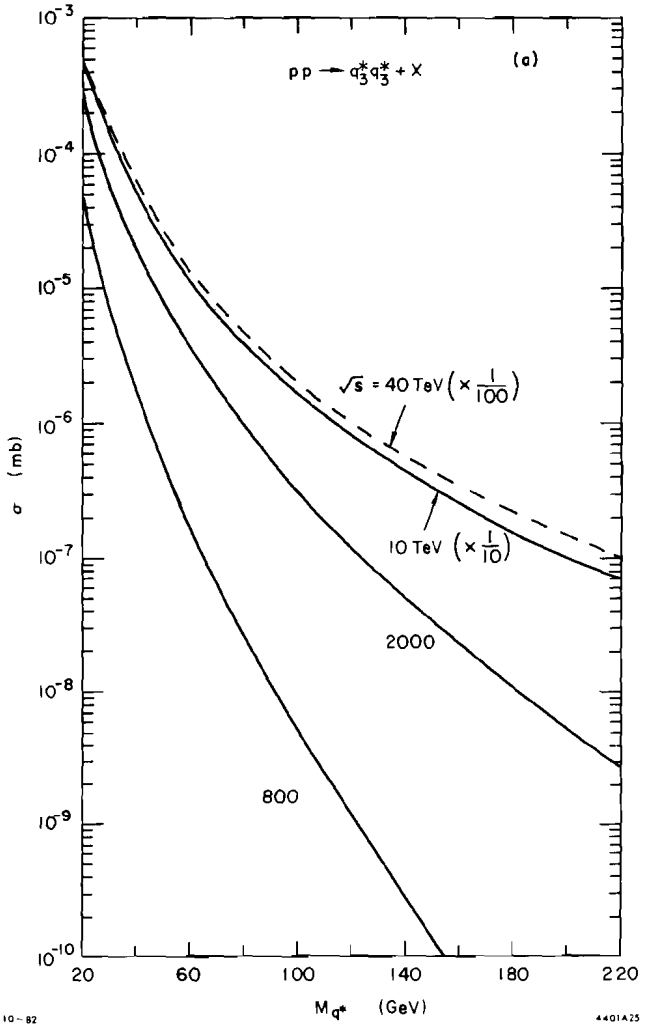

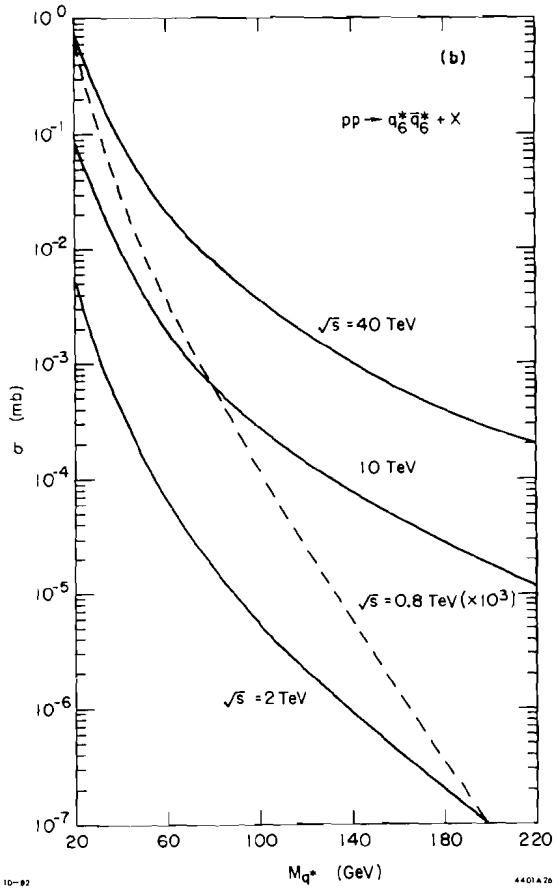

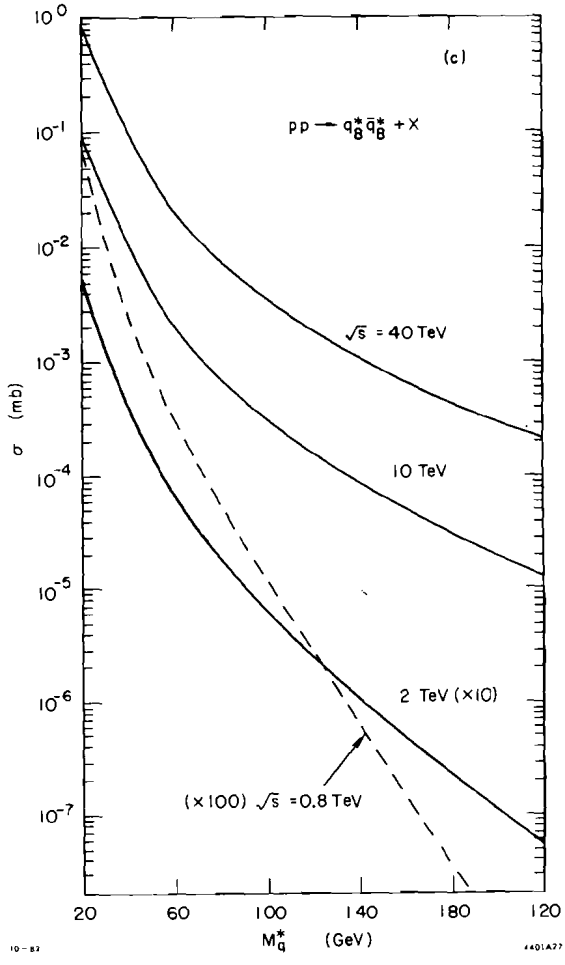

Fig. 24. Cross sections for exotic fermion pair production in pp or $p\bar{p}$ collisions, for various values of s. The various plots show results for fermions which are: a) color triplet (excited quarks); b) color sextet; c) color octet.

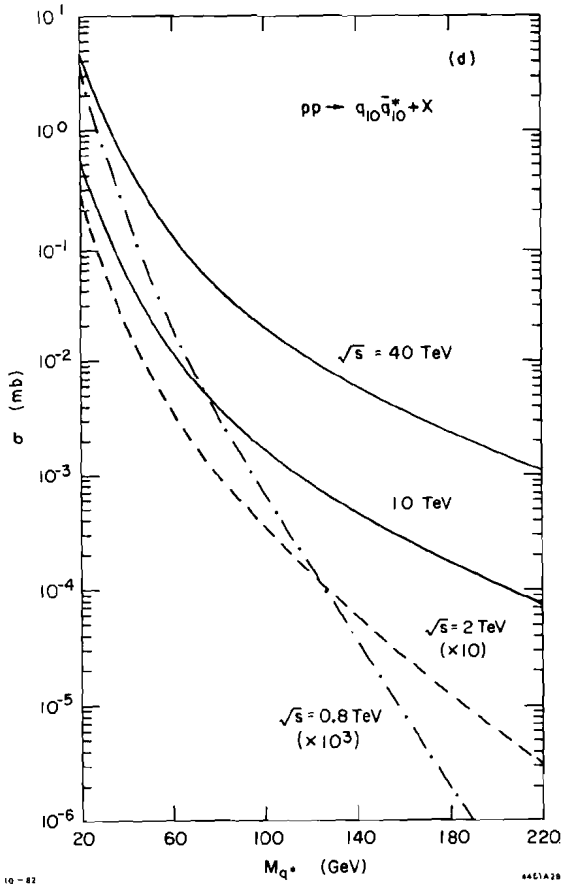

Fig. 24. Cross sections for exotic fermion pair production in pp or $p\bar{p}$ collisions, for various values of s. The various plots show results for fermions which are: d) color decouplet.

This simple rule shows, e.g., that for equal masses, color decuplet (10) quarks are produced 360/(16/3) = 67.5 times more copiously than ordinary color triplet (3) quarks.

(iii) Signatures and Detection

We now briefly comment on the various signatures for the detection of these objects. The excited leptons will most likely decay to a photon and an ordinary lepton. Depending on the values of Λ, these leptons will have lifetimes ranging over a wide region. Hence one should look for low multiplicity events with photons or heavy tracks in e^+e^- collisions.

In the case of an "octet-lepton," the signature will be dramatic if the excited leptons are pair produced in hadronic collisions and Λ is small enough. Each fermion will decay back into a lepton and a jet, leading to very stiff leptons recoiling against jets. The stiffness of the lepton should allow one to distinguish it from a normal heavy-quark lepton. Again, if Λ is large enough this object would be long-lived.

The case of color triplet, sextet and octet quarks can be discussed simultaneously. For small enough Λ, they will be simply produced and decay back into a quark and a gluon, leading to two back-to-back jets. In this case their detection must rely on jet mass reconstruction, as in the $W^{\pm}$ hadronic decay modes. If Λ is large, they will be doubly produced by longer-lived; it is likely that they will decay at a vertex visibly (mm - cm) separated from the interaction vertex. The most interesting candidate is the color decuplet quark. It is always pair produced, and cannot decay because of the color factors. So here we must look for a long-lived hadron, which can be either charged or neutral.

As we can see from this brief survey, the situation for experimenters will be difficult on the whole. One must hope that Λ is either very small, to allow unusual processes, or very large, to make these new states essentially stable. One can only trust one's luck, and look.

Appendix A

In this section we present the most general 4-fermion interaction satisfying the constraints of flavor and SU(2) × U(1) conservation. Since this table is meant to be illustrative rather than being a basis of calculations, we restrict ourselves to interactions involving leptons only. For interactions involving $e_R, \nu_R, L_a = (\nu, e)_L$ only:

$$\begin{aligned}\delta\mathcal{L} = \frac{1}{\Lambda^2}\Big\{ & a_1\,\bar{L}_a\gamma^\mu L_a\,\bar{L}_b\gamma_\mu L_b \\ & + a_2\,(\bar{e}_R\gamma^\mu e_R)(\bar{e}_R\gamma_\mu e_R) \\ & + a_3\,(\bar{\nu}_R\gamma^\mu\nu_R)(\bar{e}_R\gamma_\mu e_R) \\ & + a_4\,(\bar{\nu}_R\gamma^\mu e_R)(\bar{e}_R\gamma_\mu\nu_R) \\ & + a_5\,(\bar{L}^a\gamma^\mu L^a)(\bar{e}_R\gamma^\mu e_R) \\ & + a_6\,(\bar{L}^a\gamma^\mu L^a)(\bar{\nu}_R\gamma^\mu\nu_R) \\ & + a_7\left[\varepsilon_{ab}(\bar{L}^a\nu_R)(\bar{L}^b e_R) + \text{h.c.}\right]\Big\}\end{aligned} \tag{A.1}$$

For interactions involving two different leptons: ℓ_{iR}, ν_{iR}, L_i; i = R,μ,τ

$$\begin{aligned}\delta\mathcal{L} = \frac{1}{\Lambda^2}\Big\{ & b_1(\bar{L}_1^a\gamma^\mu L_1^a)(\bar{L}_2^b\gamma_\mu L_2^b) \\ & + b_2\,(\bar{L}_1^a\gamma^\mu L_1^b)(\bar{L}_2^b\gamma_\mu L_2^a) \\ & + b_3\,(\bar{\ell}_{1R}\gamma^\mu\ell_{1R})(\bar{\ell}_{2R}\gamma_\mu\ell_{2R}) \\ & + b_4\,(\bar{\nu}_{1R}\gamma^\mu\nu_{1R}\,(\bar{\nu}_{2R}\gamma_\mu\nu_{2R}) \\ & + b_5\left\{(\bar{\nu}_{1R}\gamma^\mu\ell_{2R})(\bar{\ell}_{2R}\gamma_\mu\nu_{1R}) + (1\leftrightarrow 2)\right\} \\ & + b_6\left\{(\bar{L}_1^a\gamma^\mu L_1^a)(\bar{\ell}_{2R}\gamma^\mu\ell_{2R}) + (1\leftrightarrow 2)\right\} \\ & + b_7\left\{(\bar{L}_1^a\gamma^\mu L_2^a)(\bar{\nu}_{2R}\gamma^\mu\nu_{2R}) + (1\leftrightarrow 2)\right\} \\ & + b_8\left\{(\bar{L}_1^a\gamma^\mu L_2^a)(\bar{\ell}_{2R}\gamma_\mu\ell_{1R}) + (1\leftrightarrow 2)\right\} \\ & + b_9\left\{(\bar{L}_1^a\gamma^\mu L_2^a)(\bar{\nu}_{2R}\gamma_\mu\nu_{1R}) + (1\leftrightarrow 2)\right\} \\ & + b_{10}\left\{\varepsilon_{ab}(\bar{L}_1^a\nu_{1R})(\bar{L}_2^b\ell_{2R}) + (1\leftrightarrow 2)\right\} \\ & + b_{11}\left\{\varepsilon_{ab}(\bar{L}_1^a\nu_{2R})(L_2^b\ell_{1R}) + (1\leftrightarrow 2)\right\}\Big\}\,.\end{aligned} \tag{A.2}$$

Helicity conservation may require that a_7, b_{10}, and b_{11} be set to zero.

Appendix B

It is straightforward to work out the modification of the usual formulae for parton-model processes in the presence of the contact interaction (10). We will simply record the results here.

For each flavor of fermion, define functions $A_f(s)$, $B_f(s)$ as follows:

for $f = e,\mu,\tau$

$$A_f(s) = \left(1 + \frac{(1/2 - \sin^2\theta_w)}{\sin^2\theta_w\cos^2\theta_w}\frac{s}{s - m_Z^2} + \frac{A_1 s}{\alpha\Lambda^2}\right)^2 + \left(1 + \frac{\sin^4\theta_w}{\sin^2\theta_w\cos^2\theta_w}\frac{s}{s - m_Z^2}\right)^2 \qquad (B.1)$$

$$B_f(s) = 2\left(1 - \frac{\sin^2\theta_w(1/2 - \sin^2\theta_w)}{\sin^2\theta_w\cos^2\theta_w}\frac{2}{s - m_Z^2}\right)^2$$

for $f = u,c,t$ (above threshold)

$$A_f(s) = 3\left[\left(\frac{2}{3} + \frac{(\frac{1}{2} - \frac{2}{3}\sin^2\theta_w)(\frac{1}{2} - \sin^2\theta_w)}{\sin^2\theta_w\cos^2\theta_w}\frac{s}{s - m_Z^2} + \frac{A_2 s}{\alpha\Lambda^2}\right)^2 + \left(\frac{2}{3} + \frac{\frac{2}{3}\sin^4\theta_w}{\sin^2\theta_w\cos^2\theta_w}\frac{s}{s - m_Z^2}\right)^2\right] \qquad (B.2)$$

$$B_f(s) = 3\left[\left(\frac{2}{3} - \frac{\frac{2}{3}\sin^2\theta_w(\frac{1}{2} - \sin^2\theta_w)}{\sin^2\theta_w\cos^2\theta_w}\frac{s}{s - m_Z^2}\right)^2 + \left(\frac{2}{3} - \frac{\sin^2\theta_w(\frac{1}{2} - \frac{2}{3}\sin^2\theta_w)}{\sin^2\theta_w\cos^2\theta_w}\frac{s}{s - m_Z^2}\right)^2\right]$$

and for $f = d,s,b$

$$A_f(s) = 3\left[\left(\frac{1}{3} + \frac{(\frac{1}{2} - \frac{1}{3}\sin^2\theta_w)(\frac{1}{2} - \sin^2\theta_w)}{\sin^2\theta_w\cos^2\theta_w}\frac{s}{s - m_Z^2} + \frac{A_3 s}{\alpha\Lambda^2}\right)^2 + \left(\frac{1}{3} + \frac{\frac{1}{3}\sin^4\theta_w}{\sin^2\theta_w\cos^2\theta_w}\frac{s}{s - m_Z^2}\right)^2\right] \qquad (B.3)$$

$$B_f(s) = 3\left[\left(\frac{1}{3} - \frac{\frac{1}{3}\sin^2\theta_w(\frac{1}{2} - \sin^2\theta_w)}{\sin^2\theta_w\cos^2\theta_w}\frac{s}{s - m_Z^2}\right)^2 + \left(\frac{1}{3} - \frac{\sin^2\theta_w(\frac{1}{2} - \frac{1}{3}\sin^2\theta_w)}{\sin^2\theta_w\cos^2\theta_w}\frac{s}{s - m_Z^2}\right)^2\right]$$

then:

(1) If $f \neq e$, the e^+e^- cross section for producing $f\bar{f}$ is:

$$\frac{d\sigma}{d\Omega}(e^+e^- \to f\bar{f}) = \frac{\alpha^2}{16s}\left[(1 + \cos\theta)^2 A_f(s) + (1 - \cos\theta)^2 B_f(s)\right] . \qquad (B.4)$$

(2) If f is a quark flavor, the ep (or μp) deep inelastic scattering cross section is given by

$$\frac{d^2\sigma}{dxdy} = \frac{\pi\alpha^2}{\delta x^2 y^2}\sum_f\left[xf_f(x)\left\{\frac{1}{3}A_f(-Q^2) + (1 - y)^2\cdot\frac{1}{3}B_f(-Q^2)\right\} + xf_{\bar{f}}(x)\left\{\frac{1}{3}B_f(-Q)^2 + (1-y)^2\frac{1}{3}A_f(-Q)^2\right\}\right] \qquad (B.5)$$

where $Q^2 = xys$.

(3) The parton subprocess cross sections for $q\bar{q} \to \mu^+\mu^-$ are

$$\frac{d\hat{\sigma}}{d\hat{t}} = \frac{\pi\alpha^2}{3\hat{s}^2}\left[\frac{1}{3}A_f(\hat{s})\left(\frac{\hat{u}}{\hat{s}}\right)^2 + \frac{1}{3}B_f(\hat{s})\left(\frac{\hat{t}}{\hat{s}}\right)^2\right] \qquad (B.6)$$

and

$$\hat{\sigma} = \frac{\pi\alpha^2}{27\hat{s}}\left[A_f(\hat{s}) + B_f(\hat{s})\right] \qquad (B.7)$$

(4) The Bhabha scattering cross section can be expressed as

$$\frac{d\sigma}{d\Omega}(e^+e^- \to e^+e^-) = \frac{\alpha^2}{16s}\left[(1 + \cos\theta)^2 A(s) + (1 - \cos\theta)^2 B(s) + 8\,C(s)\right] \qquad (B.8)$$

where

$$A(s) = \left\{\left(1 + \frac{(\frac{1}{2} - \sin^2\theta_w)^2}{\sin^2\theta_w\cos^2\theta_w}\frac{s}{s - m_Z^2} + 2\frac{A_1 s}{\alpha\Lambda^2}\right) + \frac{s}{t}\left(1 + \frac{(\frac{1}{2} - \sin^2\theta_w)^2}{\sin^2\theta_w\cos^2\theta_w}\frac{t}{t - m_Z^2}\right)\right\}^2 + \left\{\left(1 + \frac{\sin^4\theta_w}{\sin^2\theta_w\cos^2\theta_w}\frac{s}{s - m_Z^2}\right) + \frac{s}{t}\left(1 + \frac{\sin^4\theta_w}{\sin^2\theta_w\cos^2\theta_w}\frac{t}{t - m_Z^2}\right)\right\}^2$$

$$B(s) = 2\left(1 - \frac{\sin^2\theta_w(\frac{1}{2} - \sin^2\theta_w)}{\sin^2\theta_w\cos^2\theta_w}\frac{s}{s - m_Z^2}\right)^2$$

$$C(s) = \left(\frac{s}{t}\right)^2\left\{1 - \frac{(\frac{1}{2} - \sin^2\theta_w)}{\cos^2\theta_w}\frac{t}{t - m_Z^2}\right\}^2$$

5) Finally the various cross sections for QCD hard scattering (single gluon exchange) are tabulated as modified by the introduction of a contact term

$$\frac{4\pi A}{2\Lambda^2}\left(\bar{u}_L\gamma^\mu u_L + \bar{d}_L\gamma^\mu d_L\right)\left(\bar{u}_L\gamma_\mu u_L + \bar{d}_L\gamma_\mu d_L\right) \tag{B.9}$$

$$\frac{d\hat{\sigma}^{ij}}{d\hat{t}} = \frac{\pi}{\hat{s}^2}\,|A^{ij}|^2 \qquad \hat{u}+\hat{t}+\hat{s}=0$$

	Subprocess	$\lvert A^{ij}\rvert^2$
a)	$u\bar{u} \to u\bar{u}$ (or $d\bar{d} \to d\bar{d}$)	$\frac{4}{9}\left[(\hat{u}^2+\hat{s}^2)\left(\frac{\alpha(\hat{t})}{\hat{t}}\right)^2 + (\hat{u}^2+\hat{t}^2)\left(\frac{\alpha(\hat{s})}{\hat{s}}\right)^2\right]$ $- \frac{8}{27}\frac{\alpha(\hat{t})}{\hat{t}}\frac{\alpha(\hat{s})}{\hat{s}}\hat{u}^2 + \frac{8}{9}\frac{\hat{u}^2}{\Lambda^2}A\left[\frac{\alpha(\hat{t})}{\hat{t}}+\frac{\alpha(\hat{s})}{\hat{s}}\right]$ $+ \frac{8}{3}\left(\frac{1}{\Lambda^2}\right)^2\hat{u}^2A^2$
b)	$uu \to uu$ (or $dd \to dd$)	$\frac{4}{9}\left[(\hat{u}^2+\hat{s}^2)\left(\frac{\alpha(\hat{t})}{\hat{t}}\right)^2 + (\hat{t}^2+\hat{s}^2)\left(\frac{\alpha(\hat{u})}{\hat{u}}\right)^2\right]$ $- \frac{8}{27}\hat{s}^2\frac{\alpha(\hat{t})}{\hat{t}}\frac{\alpha(\hat{u})}{\hat{u}} + \frac{8}{9}\frac{\hat{s}^2}{\Lambda^2}A\left(\frac{\alpha(\hat{t})}{\hat{t}}+\frac{\alpha(\hat{u})}{\hat{u}}\right)$ $+ \left(\frac{1}{\Lambda^2}\right)^2A^2\left(\hat{u}^2+\hat{t}^2+\frac{2}{3}\hat{s}^2\right)$
c)	$ud \to ud$ (or $u\bar{d} \to u\bar{d}$, $\bar{u}d \to \bar{u}d$, $\bar{u}\bar{d} \to \bar{u}\bar{d}$)	$\frac{4}{9}\left[\hat{u}^2+\hat{s}^2\right]\left(\frac{\alpha(\hat{t})}{\hat{t}}\right)^2 + \left(\frac{1}{\Lambda^2}\right)^2A^2\hat{u}^2$
d)	$u\bar{u} \to d\bar{d}$ (or $d\bar{d} \to u\bar{u}$)	$\frac{4}{9}\left[\hat{u}^2+\hat{t}^2\right]\left(\frac{\alpha(\hat{s})}{\hat{s}}\right)^2 + \left(\frac{1}{\Lambda^2}\right)^2A^2\hat{u}^2$

while the two subprocesses $qg \to qg$ and $gg \to q\bar{q}$ are unmodified by the contact interaction

e)	$ug \to ug$ (or $dg \to dg$, $\bar{u}g \to \bar{u}g$, $\bar{d}g \to \bar{d}g$)	$-\frac{4}{9}(\hat{u}^2+\hat{s}^2)\left[\frac{\alpha(\hat{u})}{\hat{u}}\frac{\alpha(\hat{s})}{\hat{s}}\right]$ $+ \left(\frac{\alpha(\hat{t})}{\hat{t}}\right)^2(\hat{u}^2+\hat{s}^2)$
f)	$gg \to u\bar{u}$ (or $gg \to d\bar{d}$)	$\frac{1}{6}(\hat{u}^2+\hat{t}^2)\frac{\alpha(\hat{u})}{\hat{u}}\frac{\alpha(\hat{t})}{\hat{t}}$ $- \frac{3}{8}(\hat{u}^2+\hat{t}^2)\left(\frac{\alpha(\hat{s})}{\hat{s}}\right)^2$

References

1. M. E. Peskin, in Proc. of the 1981 Int. Symp. on Lepton and Photon Interactions at High Energy, W. Pfeil, ed. (Bonn, 1981), pp. 880.

2. K. M. Case and S. Gasiorowicz, Phys. Rev. 125, 1055 (1962); L. Durand, Phys. Rev. 128, 434 (1962); S. Weinberg and E. Witten, Phys. Lett. 96B, 59 (1980).

3. J. Branson, in Proc. of the 1981 Int. Symp. on Lepton and Photon Interactions at High Energy, W. Pfeil, ed. (Bonn, 1981), pp. 279.

4. J. Calmet, S. Narison, M. Perrottet, and E. deRafael, Rev. Mod. Phys. 49, 21 (1977); T. Kinoshita and W. B. Lindquist, Phys. Rev. Lett. 47, 1573 (1981).

5. R. Barbieri, L. Maiani, and R. Petronzio, Phys. Lett. 96B, 63 (1980); S. J. Brodsky and S. D. Drell, Phys. Rev. D 22, 2236 (1980).

6. K. V. Klitzing, G. Dorda, and M. Pepper, Phys. Rev. Lett. 45, 494 (1980); E. Braun et al., and C. Yamagouchi, et al., in Proc. of the Second Int. Conf. on Precision Measurement and Fundamental Constants, B. N. Taylor and W. D. Phillips, eds. (National Bureau of Standards, 1981).

7. P. B. Schwinberg, R. S. Van Dyck, Jr., and G. H. Dehmelt, Phys. Rev. Lett. 47, 1679 (1981).

8. T. Kinoshita, contribution to the Fifth Int. Symp. on High Energy Spin Physics, Brookhaven National Laboratory, 16-22 September 1982.

9. W. Lee, R. Wilson, et al., Fermilab Proposal 708.

10. A. DeRujula, Phys. Lett. 65B, 279 (1980).

11. E. Eichten, K. Lane, and M. Peskin submitted for publication.

12. D. P. Barber et al., Phys. Rev. Lett. 46, 1663 (1981).

13. J. Leveille, University of Michigan Preprint UM-HE8220 (1982).